Progress in Natural Science: Materials International 26 (2016) 422–426

HOSTED BY

Contents lists available at ScienceDirect

Progress in Natural Science: Materials International

journal homepage: www.elsevier.com/locate/pnsmi

Graphene/$SrTiO_3$ hetero interface studied by X-ray photoelectron spectroscopy

S. Karamat [a,d,*], C. Ke [b], U.Y. Inkaya [a], Rizwan Akram [c], Ilker Yildiz [a], S. Shah Zaman [d], A. Oral [a,*]

[a] Department of Physics, Middle East Technical University, Ankara 06800, Turkey
[b] Microelectronics Centre, School of Electrical and Electronic Engineering, Nanyang Technological University, 639798, Singapore
[c] Department of Electrical Engineering, College of Engineering, Qassim University, Saudi Arabia
[d] COMSATS Institute of Information Technology, Islamabad 54000, Pakistan

ARTICLE INFO

Article history:
Received 21 November 2015
Received in revised form
28 June 2016
Accepted 29 June 2016
Available online 20 August 2016

Keywords:
Chemical vapour deposition
X-ray photoelectron spectroscopy
Raman spectroscopy
Graphene
Valence band maximum

ABSTRACT

The present paper focuses on study of graphene and strontium titanate ($SrTiO_3$ or STO) interface. An ambient pressure chemical vapour deposition (AP-CVD) setup is used to grow graphene on STO (110) substrates in the presence of methane, argon and hydrogen gases at 1000 °C for 4 h. Raman spectroscopy measurements confirm the presence of graphene on STO substrates due to the existence of typical D and G peaks referring to graphene. These characteristic peaks are missing in the spectrum for bare substrates. X-ray photoelectron spectroscopy (XPS) is carried out for elemental analysis of samples, and study their bonding with STO substrates. We employed the valence band spectrum to calculate the valence band offset (VBO) and conduction band offset (CBO) at the G-STO interface. Also, we present an energy band diagram for Bi-layer and ABC (arranging pattern of carbon layers) stacked graphene layers.

1. Introduction

The diversity required in designing electronic devices keeps motivating researchers from across the globe to study new functional materials and device structures. Graphene, a monolayer of sp2 bonded carbon atom, is potentially an ideal candidate for a wide range of applications in electronics [1,2]. A number of methods like exfoliation of graphite via scotch tape [3], reduction of graphene oxide [4], decomposition of hydrocarbons via CVD [5,6] and plasma enhanced chemical vapour deposition (PECVD) [7,8] have been used to synthesize graphene, and further transfer it to the desired substrate for device fabrication. The most critical step in graphene research is its transfer from the growth catalyst to the dielectric substrate. A few of many ineluctable challenges commonly faced during the transfer process are: contamination from etchants, photoresist residues, wrinkles, and mechanical breakage. Few attempts have been made to grow graphene directly on the insulating substrates such as $SrTiO_3$ [9], MgO [10,11], SiO_2 [12–14], Al_2O_3 [15,16], Si_3N_4 [17,18] etc. by CVD. The direct growth of graphene on the substrates without using a catalyst, offers new opportunities in device fabrication in addition to avoid the issues related to any transfer process. Until recently, the field of direct graphene growth on dielectrics or insulating substrates is not developed enough like the growth on metallic catalysts using CVD. Therefore, more study is in high demand regarding the understanding of substrate and graphene interface, crystal quality, chemical composition, band alignment and graphene substrate bonding.

It is important to select an appropriate insulating substrate because their downscaling in device fabrication alters their properties. For example, in graphene-based field effect transistor, the insulating substrate (SiO_2) is mostly used as a gate electrode and it faces a predicament about scattering of carriers and leakage current, which affects the final output of the device functioning. To avoid leakage problem and improve gate modulation, it is always advisable to choose the high K-dielectric substrates. Different phenomena like quasi-two dimensional electron gases [19], tunable ferromagnetism [20], colossal magneto-resistance [21], and superconductivity [22] were observed in the dielectric perovskite complex oxide device structures. The combination of graphene with such materials is a promising research approach from both perspectives; theoretical and experimental. The wide spectra of physical properties of dielectric perovskites make an interesting contribution in graphene based hetero-structure devices.

* Corresponding authors.
E-mail addresses: shumailakaramat@gmail.com (S. Karamat), orahmet@metu.edu.tr (A. Oral).
Peer review under responsibility of Chinese Materials Research Society.

http://dx.doi.org/10.1016/j.pnsc.2016.06.010

2. Experimental

Graphene is grown on $SrTiO_3$ (110) substrates in an ambient pressure CVD (AP-CVD) setup. The substrates are cleaned with acetone, isopropanol and deionised (DI) water followed by blow drying. The cleaned substrates are then, placed in the quartz reaction chamber, and the setup is evacuated down to a pressure of $\sim 5 \times 10^{-2}$ mbars. The chamber consists of a 40 mm diameter quartz tube reaction chamber mounted on a split CVD furnace. Continuous flow of high purity reaction gases: CH_4 [99.995% purity, Messer], H_2 [99.999% purity, BOS] and Argon [99.999% purity, Messer] is used for the growth of graphene layer on substrate. Ar gas is used to flush the system at a flow rate of 300 sccm followed by the hydrogen gas at the rate of 50 sccm before the furnace temperature ramps. The furnace is turned on and its temperature is ramped upto 1000 °C, the Ar flow is maintained at 100 sccm throughout the experiment. When the furnace temperature reaches 1000 °C and is stable, H_2 (50 sccm) and CH_4 (8 sccm) gases are introduced in the reaction chamber. Graphene growth lasts for 4 h. The furnace lid is opened immediately, as soon as the growth finishes. CH_4 flow is discontinued when the temperature falls to 650 °C. The samples are cooled down to room temperature in an Ar and H_2 atmosphere. Renishaw inVia Reflex microRaman spectrometer with 532 nm laser source is used to measure the Raman spectra. Phi Versaprobe is equipped with UPS X-ray photoelectron spectroscope is used, and spectra are recorded using monochromatic Al K_α radiation [1486.6 eV].

3. Results and discussion

Raman spectroscopy is extensively used for the characterization of graphitic materials. The characteristic bands of graphene like D, G and 2D provide valuable information about the defects, in-plane vibration of sp2 carbon atoms and the stacking orders, respectively [23,24]. Raman spectroscopy is performed on bare and graphene grown STO substrates. The as grown graphene-STO (G-STO) substrate shows the appearance of D and G peak around 1297.24 cm^{-1} and 1597.5 cm^{-1} respectively, which are absent in the bare STO substrates, as shown in the inset of Fig. 1. The 2D peak is not observed, which might have been due to substrate screening effect. The strain developed due to lattice mismatch or the stronger interactions between carbon and STO bonds may cause the screening effect [9]. The suppression of 2D peak is also observed in the case of SiC [24]. The intensity ratio of D to G peak is usually employed to estimate the disorder found in graphene, which is in direct measure of its quality. For present investigation, the I_D/I_G ratio is found to be 0.3, larger than the reported value in previous studies [25,26]. This larger ratio can be attributed to the presence of nano-graphene with greater disorder. To confirm the existence of graphene, the XPS spectrum of G-STO is de-convolved using Gaussian peak fit, and found that the binding energy of carbon content is of sp2 carbon (graphene) as shown in Fig. 2f.

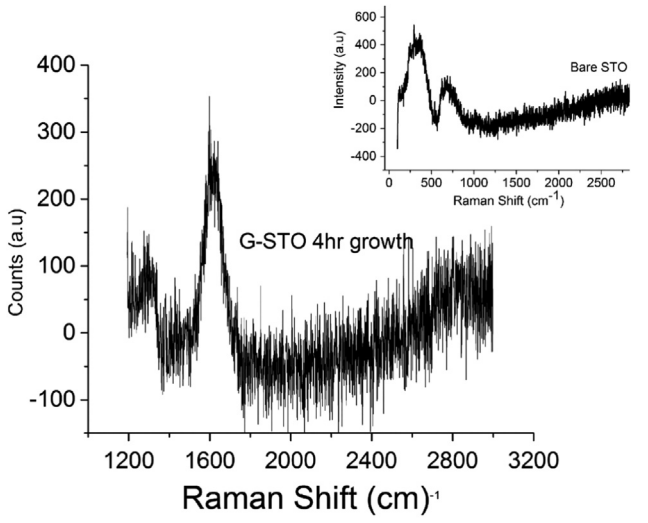

Fig. 1. Raman Spectrum of graphene on STO substrates for 4 h growth, Inset shows the Raman Spectrum of bare STO for comparison.

XPS is used to get information about the interaction between the C1s and the STO substrates, shown in Fig. 2. Moreover, XPS gives the information about the valence and conduction band offsets at the interface, which is a very pertinent information for the device structure. C1s and Ti2p core peaks of bare STO, STO heated at 1000 °C before growth, G-STO sample after growth clearly indicate the change in binding energy. Fig. 2e, shows C1s peak for graphene, for the sample grown for 4 h on STO substrates, appearing at around 285.3 eV. Whereas the binding energy of standard highly ordered pyrolytic graphite (HOPG) sample is about 284.3 eV. The C1s peak of as-grown G-STO substrate is quite broad which shows the interaction of the substrate elements with carbon. In order to get the information about the interaction of different substrate elements with carbon, C1s core peak is de-convolved into three Gaussians having peaks at 284.6, 285.3 and 285.9 eV. The resultant peak around 284.6 eV is identified as the graphitic (sp2) non-oxygenated C ring (C–C, 284.6 ± 0.2 eV) [27,28]. The other two peaks represent sp3 and bonding with other elements like hydrogen and oxygen [9,27]. The residual C1s for bare and heated STO substrates show carbon peak around 283.07 eV, which is a confirmation of carbon and titanium bonding [9].

Ti 2p doublets for bare and bare heated STO substrate along with G-STO substrate core level spectrum are shown in Fig. 2d. According to literature, the doublets at 454.7 eV and 460.6 eV belong to TiC ($2p_{1/2}$ and $2p_{3/2}$) [29], and the peaks appearing at 458.3 eV and 464 eV are assigned to TiO_2 [30]. Moreover, a combination of oxide and carbon with titanium (sub-stoichiometric TiCx($x < 1$) and TiOx(or TiCxO)) also exist, and these peaks appear around 456.2 eV and 462 eV [31]. The Ti $2p_{1/2}$ and $2p_{3/2}$ peaks of the TiC phase shifted towards higher binding energies relative to the elemental Ti 2p (453.8 and 459.9 eV) peaks in elemental Ti 2p, due to a chemical shift, resulting from charge transfer and mixed bonding [32]. In the present case, $Ti2p_{3/2}$ and $Ti2p_{1/2}$ core peaks for G-STO sample appeared around 459.0 and 464.8 eV respectively, and show a shift of 2.6 eV towards higher binding energy from bare substrates due to carbon and oxygen bonding.

XPS is a powerful tool to give the information about the band offsets in semiconductors and the valence band (VB) discontinuities of heterojunctions [33–37]. In our samples, the XPS data has been used to obtain the information about the band alignment at the graphene-STO interface. The information about the band alignment at interfaces, particularly the valence band offset (VBO) and conduction band offset (CBO) are critical in understanding and designing the electronic properties of device structures. To determine the VBO of graphene/STO interface the high-resolution XPS spectra of VB, C1s and Ti 2p core levels is obtained from G-STO, HOPG, and heated bare STO substrates. The VBO can be calculated by applying the following formula [38,39]:

$$\Delta E_v = \Delta E_{CL} + (E_{C1s}^{HOPG} - E_{VBM}^{HOPG}) - (E_{Ti2p3/2}^{STO} - E_{VBM}^{STO}) \quad (1)$$

where $\Delta E_{CL} = E_{Ti2p3/2}^{G-STO\ substrate} - E_{C1s}^{G-STO\ substrate}$ is the binding energy difference between $Ti2p_{3/2}$ and C1s core level spectra for the 4 h graphene growth on STO substrate, $E_{C1s}^{HOPG} - E_{VBM}^{HOPG}$ is the binding energy difference between C1s and valence band maximum obtained from the HOPG, and $E_{Ti2p3/2}^{STO} - E_{VBM}^{STO}$ is the binding energy

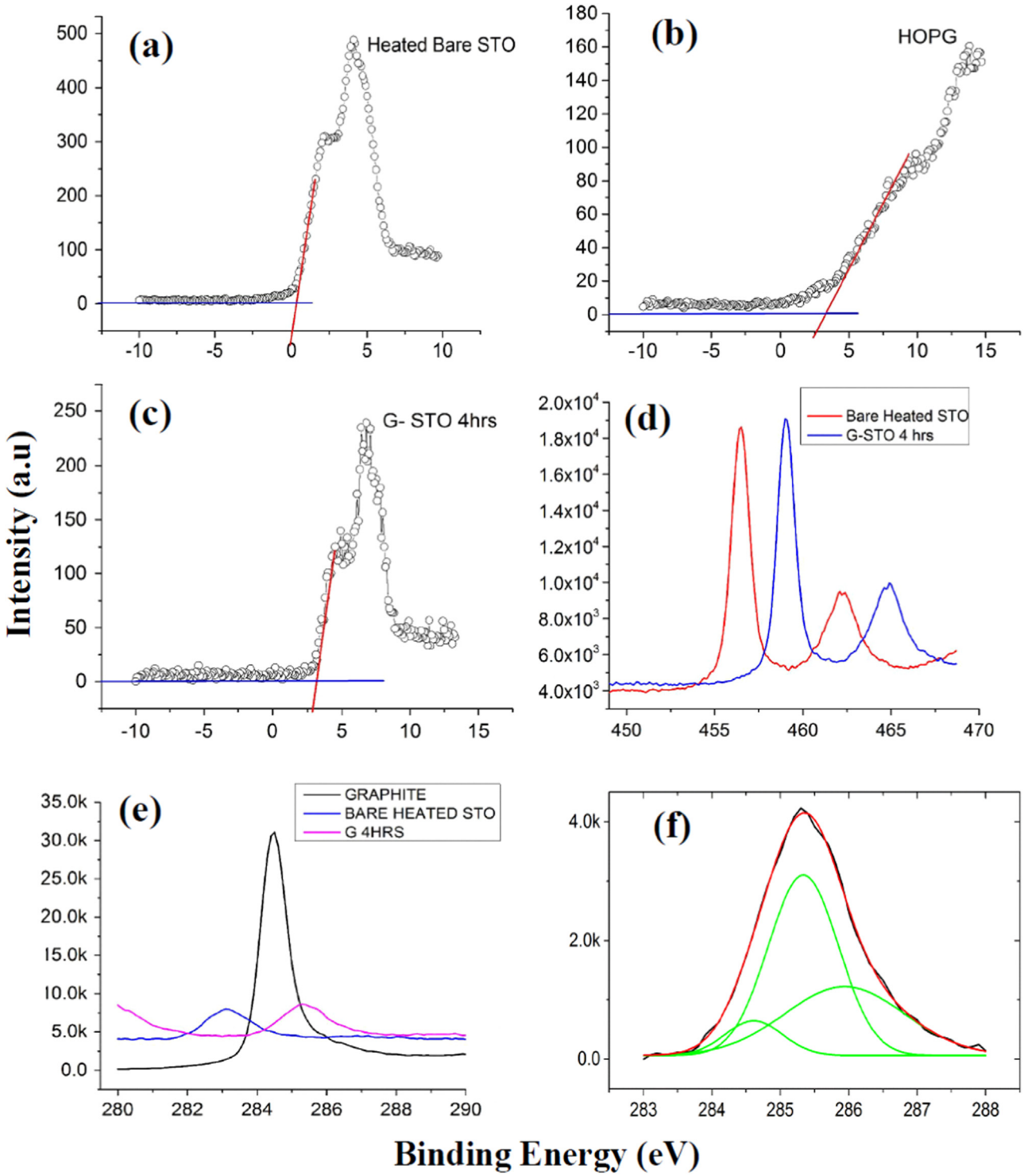

Fig. 2. XPS valence band obtained for three samples (a) Bare heated STO, (b) Graphite (HOPG), (c) G-STO for 4 h growth, (d)Ti 2p doublets for Bare heated STO and 4 h G-STO, (e) core-level spectra of C1s for Bare heated substrate, Graphite and 4 h G-STO, (f) de-convolved C1s spectrum for G-STO 4 h sample.

Table 1
Binding energies of the valence band maximum, C1s, and Ti $2p_{3/2}$ core-level spectra obtained from the three samples.

Samples	VBM	C1s	Ti$2p_{3/2}$
G-STO	–	285.3	459.04
HOPG	3.31	284.48	–
Bare heated substrate	0.38	–	456.49

difference between Ti$2p_{3/2}$ and VBM of the heated bare STO substrate. The core-level and VB XPS spectra of G-STO, HOPG, heated bare STO samples are shown in Fig. 2. The valence band maximum (VBM) values are derived by extrapolating a linear fit to the leading edge of the VB spectra with respect to the background level. Table 1 shows the binding energy of the spectra shown in Fig. 2.

By substituting these values into Eq. (1) the VBO of graphene/STO hetero-interface is calculated to be −1.02 eV, which means

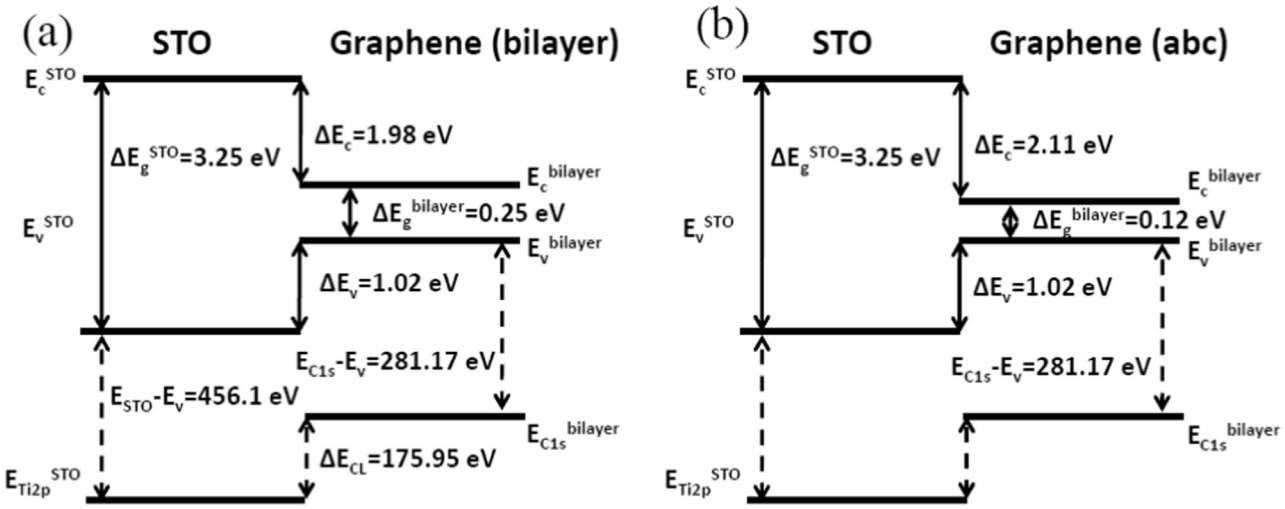

Fig. 3. Schematic energy band diagram of the G/$SrTiO_3$ hetero interface.

that the VBM of graphene is lower than that of STO. In addition, the CBO (ΔE_C) can be estimated by the following formula:

$$\Delta E_C = \Delta E_v + E_g^G - E_g^{STO} \quad (2)$$

By using, the room-temperature energy band gap values (E_g^{STO} and E_g^G), as reported in the literature [40–42], the ΔE_C is calculated to be 1.98 eV for bilayer and 2.11 eV for ABC stacked graphene layers. On the basis of aforementioned analysis, the energy band diagram is illustrated in Fig. 3.

4. Conclusion

The study commentates on the band alignment of graphene grown on $SrTiO_3$ (110) substrates. AP-CVD set-up is used for the catalyst-free growth of graphene on STO substrates at 1000 °C for 4 h. The gases used for growth are hydrogen, methane and argon. Raman spectroscopy is used to confirm the presence of graphene due to appearance of D and G peaks. It is imperative to mention here, that the oxide content greatly influences the 2D peak appearance in Raman spectrum, which is not visible in the samples. Hence, the information regarding the number of graphene layers cannot be predicted accurately. Moreover, the presence of nano-graphene is also estimated from I_D/I_G ratio. XPS analysis has been carried out in detail, to obtain information about the bonding of different elements with STO substrates. C1s peak for graphene appears around 284.6 eV in the de-convolved spectrum of G-STO 4hr growth, which indicates sp2 carbon bonding. Ti2p core peak shows a shift of 2.6 eV towards higher binding energy in comparison to bare substrates due to carbon and oxygen bonding. Using the valence band spectra; the valence band offset and conduction band offset are calculated at the G-STO interface. The energy band diagram is also presented for the already reported Bilayer and ABC stacked graphene layers.

Acknowledgements

S. Karamat would like to thank TÜBİTAK and European Union Marie-Curie Co-Funded 2236 Fellowship for supporting this work.

References

[1] A.K. Geim, K.S. Novoselov, Nat. Mater. 6 (2007) 183–191.
[2] D. Wei, L. Xie, K. Lee, Z. Hu, S. Tan, W. Chen, C. Sow, K. Chen, Y. Liu, A.T.S. Wee, Nat. Commun. 4 (2013) 1374.
[3] K. Novoselov, A. Geim, S. Morozov, D. Jiang, Y. Zhang, S. Dubonos, I. Grigoreva, A. Firsov, Science 306 (2004) 666–669.
[4] G. Eda, G. Fanchini, M. Chhowalla, Nat. Nanotechnol. 3 (2008) 270–274.
[5] X. Li, W. Cai, J. An, S. Kim, J. Nah, D. Yang, R. Piner, A. Velamakanni, I. Jung, E. Tutuc, S.K. Banerjee, L. Colombo, R.S. Ruoff, Science 324 (2009) 1312–1314.
[6] K.S. Kim, Y. Zhao, H. Jang, S. Lee, J.M. Kim, K.S. Kim, mJ.-H. Ahn, P. Kim, J.-Y. Choi, B.H. Hong, Nature 457 (2009) 706–710.
[7] T. Terasawaa, K. Saiki, Carbon 50 (2012) 869–874.
[8] L. Zhang, Z. Shi, Y. Wang, R. Yang, D. Shi, G. Zhang, Nano Res. 4 (2011) 315–321.
[9] J. Sun, T. Gao, X. Song, Y. Zhao, Y. Lin, H. Wang, D. Ma, Y. Chen, W. Xiang, J. Wang, Y. Zhang, Z. Liu, J. Am. Chem. Soc. 136 (2014) 6574–6577.
[10] M.H. Ruemmeli, A. Bachmatiuk, A. Scott, F. Boerrnert, J.H. Warner, V. Hoffman, J.-H. Lin, G. Cuniberti, B. Buechner, ACS Nano 4 (2010) 4206.
[11] S. Kamoi, J.-Gon -Kim, N. Hasuike, K. Kisoda, H. Harima, Jpn. J. Appl. Phys. (2014) 05FD06.
[12] J. Chen, Y. Wen, Y. Guo, B. Wu, L. Huang, Y. Xue, D. Geng, D. Wang, G. Yu, Y. Liu, J. Am. Chem. Soc. 133 (2011) 17548.
[13] H. Bi, S. Sun, F. Huang, X. Xie, M.J. Jiang, Mater. Chem. 22 (2012) 411.
[14] H. Medina, Y.-C. Lin, C. Jin, C.-C. Lu, C.-H. Yeh, K.-P. Huang, K. Suenaga, J. Robertson, P.-W. Chiu, Adv. Funct. Mater. 22 (2012) 2123.
[15] M.A. Fanton, J.A. Robinson, C. Puls, Y. Liu, M.J. Hollander, B.E. Weiland, M. LaBella, K. Trumbull, R. Kasarda, C. Howsare, J. Stitt, D.W. Snyder, ACS Nano 5 (2011) 8062.
[16] Kosuke Saito, Toshio Ogino, Phys. Chem. C 118 (2014) 5523–5529.
[17] J. Chen, Y. Guo, Y. Wen, L. Huang, Y. Xue, D. Geng, B. Wu, B. Luo, G. Yu, Y. Liu, Adv. Mater. 25 (2013) 992.
[18] J. Chen, Y. Guo, L. Jiang, Z. Xu, L. Huang, Y. Xue, D. Geng, B. Wu, W. Hu, G. Yu, Y. Liu, Adv. Mater. 26 (2014) 1348.
[19] S. Thiel, G. Hammerl, A. Schmehl, C.W. Schneider, J. Mannhart, Science 313 (2006) 1942.
[20] H. Tanaka, J. Zhang, T. Kawai, Phys. Rev. Lett. 88 (2001) 027204.
[21] C.M. Xiong, Y.G. Zhao, B.T. Xie, P.L. Lang, K.J. Jin, Appl. Phys. Lett. 88 (2006) 193507.
[22] M. Ben Shalom, M. Sachs, D. Rakhmilevitch, A. Palevski, Y. Dagan, Phys. Rev. Lett. 104 (2010) 126802.
[23] M.A. Pimenta, G. Dresselhaus, M.S. Dresselhaus, L.G. Cancado, A. Jorio, R. Saito, Phys. Chem. Chem. Phys. 9 (2007) 1276.
[24] Y.Y. Wang, Z.H. Ni, T. Yu, Z.X. Shen, H.M. Wang, Y.H. Wu, W. Chen, A.T. Shen Wee, J. Phys. Chem. C 112 (2008) 10637–10640.
[25] Y.-J. Lin, J.-J. Zeng, http://dx.doi.org/10.1016/j.apsusc.2014.10.062.
[26] Z. Luo, N.J. Pinto, Y. Davila, A.T. Charlie Johnson, Appl. Phys. Lett. 100 (2012) 253108.
[27] S. Stankovich, D.A. Dikin, R.D. Piner, K.A. Kohlhaas, A. Kleinhammes, Y. Jia, et al., Carbon 45 (7) (2007) 1558–1565.
[28] T. Bansal, C.A. Durcan, N. Jain, R.B. Jacobs-Gedrim, Y. Xu, B. Yu, Carbon 55 (2013) 168–175.
[29] J. Kovac, et al., J. Appl. Phys. 86 (1999) 5566.
[30] F. Esaka, et al., J. Vac. Sci. Technol. A 15 (1997) 2521.
[31] M. Delfino, J.A. Fair, D. Hodul, J. Appl. Phys. 71 (1992) 6079.
[32] S. Zhang, Y.Q. Fu, X.L. Bui, H.J. Du, Int. J. Nanosci. 3 (6) (2004) 797–802.
[33] Q. Chen, M. Yang, Y.P. Feng, J.W. Chai, Z. Zhang, J.S. Pan, S.J. Wang, Appl. Phys. Lett. 95 (2009) 162104.
[34] C.H. Jia, Y.H. Chen, X.L. Zhou, A.L. Yang, G.L. Zheng, X.L. Liu, S.Y. Yang, Z. G. Wang, J. Phys, Appl. Phys. 42 (2009) 095305.
[35] R.Q. Zhang, P.F. Zhang, T.T. Kang, H.B. Fan, X.L. Liu, S.Y. Yang, H.Y. Wei, Q.S. Zhu, Z.G. Wang, Appl. Phys. Lett. 91 (2007) 162104.
[36] Y.F. Li, B. Yao, Y.M. Lu, B.H. Li, Y.Q. Gai, C.X. Cong, Z.Z. Zhang, D.X. Zhao, J. Y. Zhang, D.Z. Shen, X.W. Fan, Appl. Phys. Lett. 92 (2008) 192116.

[37] P.D.C. King, T.D. Veal, S.A. Hatfield, P.H. Jefferson, C.F. McConville, C.E. Kendrick, C.H. Swartz, S.M. Durbin, Appl. Phys. Lett. 91 (2007) 112103.
[38] G. Martin, A. Botchkarev, A. Rockett, H. Morkoc, Appl. Phys. Lett. 68 (1996) 2541.
[39] K. Chang, Z. Weiguang, Z. Zheng, T.E. Soon, P. Jisheng, Surf. Interface Anal. 47 (8) (2015) 824–827.
[40] K. van Benthem, C. Elsasser, R.H. French, J. Appl. Phys. 90 (2001) 6156.
[41] Y. Zhang, T.-T. Tang, C. Girit, Z. Hao, M.C. Martin, A. Zettle, M.F. Crommie, Y. R. Shen, F. Wang, Nature 459 (2009) 820–823.
[42] C.H. Lui, Z.Q. Li, K.F. Mak, E. Cappelluti, T.F. Heinz, Nature Phys. 7 (2011) 944–947.